Please cite this article in press as: Voronin et al., Preclinical studies of gene replacement therapy for CDKL5 deficiency disorder, Molecular Therapy (2024), https://doi.org/10.1016/j.ymthe.2024.07.012

Molecular Therapy
Original Article

Preclinical studies of gene replacement therapy for CDKL5 deficiency disorder

Gregory Voronin,[1,3] Jana Narasimhan,[1,3] Jamila Gittens,[1] Josephine Sheedy,[1] Philip Lipari,[1] Melinda Peters,[1] Steven DeMarco,[1] Liangxian Cao,[1] Yakov Varganov,[1] Min Jung Kim,[1] Lisset Pear,[1] Eman Fotouh,[1] Supriya Sinha,[1] Balmiki Ray,[1] Michael C. Wu,[2] Padmaja Yalamanchili,[1] Christopher Southgate,[1] Joseph Pick,[1] Khalil Saadipour,[1] Stephen Jung,[1] Jeanee Lee,[1] Anna Mollin,[1] Ellen M. Welch,[1] Zhijian Wu,[1] and Marla Weetall[1]

[1]PTC Therapeutics, Inc, 500 Warren Corporate Center Drive, Warren, NJ 07059, USA; [2]NeuroDigitech, 8400 Miramar Road, Suite 243C, San Diego, CA 092126, USA

Cyclin-dependent kinase-like 5 (CDKL5) deficiency disorder (CDD) is a rare neurodevelopmental disorder caused by a mutation in the X-linked *CDKL5* gene. CDKL5 is a serine/threonine kinase that is critical for axon outgrowth and dendritic morphogenesis as well as synapse formation, maturation, and maintenance. This disorder is characterized by early-onset epilepsy, hypotonia, and failure to reach cognitive and motor developmental milestones. Because the disease is monogenic, delivery of the *CDKL5* gene to the brain of patients should provide clinical benefit. To this end, we designed a gene therapy vector, adeno-associated virus (AAV)9.Syn.hCDKL5, in which human *CDKL5* gene expression is driven by the synapsin promoter. In biodistribution studies conducted in mice, intracerebroventricular (i.c.v.) injection resulted in broader, more optimal biodistribution than did intra-cisterna magna (i.c.m.) delivery. AAV9.Syn.hCDKL5 treatment increased phosphorylation of EB2, a bona fide CDKL5 substrate, demonstrating biological activity *in vivo*. Our data provide proof of concept that i.c.v. delivery of AAV9.Syn.hCDKL5 to neonatal male *Cdkl5* knockout mice reduces pathology and reduces aberrant behavior. Functional improvements were seen at doses of 3e11 to 5e11 vector genomes/g brain, which resulted in transfection of ≥50% of the neurons. Functional improvements were not seen at lower doses, suggesting a requirement for broad distribution for efficacy.

INTRODUCTION

Cyclin-dependent kinase-like 5 (CDKL5) deficiency disorder (CDD) is a rare neurodevelopmental disorder associated with early-onset seizures and severe developmental delays resulting in the acquisition of little to no language skills. Patients with this disorder have profound hypotonia and severe impairments in gross motor skills. Early-onset epilepsy occurs by 3 months of age in >90% of the patients.[1–3] There is no effective therapy, and anti-epileptic drugs provide only limited seizure control.

CDD arises from mutations in the X-linked cyclin-dependent kinase-like 5 (*CDKL5*) gene, leading to a loss of function. The majority of patients are female, with a *de novo* mutation occurring in the *CDKL5* gene during early embryonic development. Due to random X-inactivation in females, approximately 50% of neurons are expected to lack CDKL5 expression, while the remaining neurons exhibit normal CDKL5 expression from the wild-type (WT) allele. More rarely, males may have CDD, in which case no neurons express normal WT CDKL5 protein. Consequently, CDD is more severe in males than in females.[4]

CDKL5 is expressed predominately in neurons in both the nucleus and the cytoplasm.[5] CDKL5 is required for maintenance of the neuronal system, including arborization of neurons and synaptic formation. CDKL5 functions as a serine/threonine kinase. It is hypothesized that CDKL5 phosphorylation of microtubule and actin-binding proteins is critical to neuronal function.[6,7]

Several *Cdkl5* knockout (KO) models have been generated, including mice lacking exon 6,[8] exon 4,[9] and exon 2[10]; mice harboring a nonsense mutation (R59X)[11]; and conditional KO mice lacking *Cdkl5* in specific cell types, including those specifically lacking CDKL5 in forebrain excitatory neurons[12] or in γ-aminobutyric acid (GABA)ergic neurons.[11] These CDD mouse models recapitulate various aspects of the human disease. However, as is true for many neurodevelopmental disorders, the mouse model disease manifestations are milder than in the human disease. Male mice lacking *Cdkl5* are typically utilized, as the female mice exhibit a more subtle phenotype. The male *Cdkl5* KO mice have deficits in learning and memory, motor function, social interactions, and anxiety.[8]

Because CDD is monogenic, gene therapy could potentially be used to restore the missing gene. A preliminary proof-of-concept study has been published.[13] This study showed a reduction but not a normalization in the pathology in *Cdkl5* KO mice by using intravenous (i.v.) delivery of an adeno-associated virus (AAV)-PHP.B capsid with a modified chicken β-actin promoter at a dose of 1e12 vector genomes (vg)/animal to mice approximately 1 month old. Biodistribution of a

Received 6 January 2024; accepted 17 July 2024;
https://doi.org/10.1016/j.ymthe.2024.07.012.

[3]These authors contributed equally

Correspondence: Marla Weetall, PTC Therapeutics, Inc, 500 Warren Corporate Center Drive, Warren, NJ 07059, USA.
E-mail: mweetall@ptcbio.com

Please cite this article in press as: Voronin et al., Preclinical studies of gene replacement therapy for CDKL5 deficiency disorder, Molecular Therapy (2024), https://doi.org/10.1016/j.ymthe.2024.07.012

PHP.B capsid is reported to be 40-fold better than that of AAV9 in specific strains of mice, but not in nonhuman primates (NHPs).[14] Therefore, it is likely that biodistribution in nonclinical mouse studies might be greater than would be obtained in the clinic. Further studies by Medici et al. compared CDKL5 gene therapy with a PHP.B-based capsid delivering WT CDKL5 with a second PHP.B-based capsid delivering a secreted CDKL5-IgkTAT fusion protein capable of cross-correction.[15] In these studies, 1e12 vg/mouse was delivered by i.v. (intracarotid) injection to adult (3–4 months old) mice. The nonsecreted CDKL5 gene therapy (AAVPHP.B-CDKL5 with a modified chicken β-actin promoter) showed little to no activity with i.v. dosing, but the secreted form resulted in modest yet statistically significant improvements, but not normalization, in behavior.

Here, we assess the efficacy of a gene therapy approach after intracerebroventricular (i.c.v.) delivery. We utilized AAV9.Syn.hCDKL5, comprising an AAV9 capsid and a synapsin promoter for cerebrospinal fluid delivery. Multiple isoforms of CDKL5 have been identified with isoform 1 being predominant in the adult brain, while isoform 2 is expressed predominately in the neonatal brain and in the testes. Isoforms 1 and 2 both have been shown to be active in a cell model of CDD, although differences in their function were noted.[13] Our studies, as well as the other published gene therapy studies, utilized isoform 1 for studies using the *Cdkl5* KO mice.

The current study in mice administered the gene therapy on the first day of life, postnatal day (PND) 0. I.c.v. dosing rather than i.v. administration allows for lower doses relative to those needed for systemic administration.

Comparing i.c.v. and intra-cisterna magna (i.c.m.) biodistribution of this AAV9-based gene therapy in mice, we show that i.c.v. results in broader biodistribution. We demonstrate dose-dependent correction of neuronal architecture and a dose-dependent reduction in aberrant behavior in the *Cdkl5* KO mouse after i.c.v. delivery of the gene therapy and correlate this with expression of CDKL5 protein and biodistribution. We demonstrate that i.c.v. administration of AAV9.Syn.hCDKL5 resulted in broad distribution throughout the brain not only in *Cdkl5* KO mice injected at PND0 but also in NHPs. In totality, our studies indicate the potential for CDKL5 gene therapy but also highlight a need for broad distribution of the vector in the brain for optimal effect.

RESULTS

Optimization of vector and route of administration

Preclinical investigations indicate widespread expression of the CDKL5 protein throughout the brain, albeit predominately limited to neurons in adult mice.[5] In the clinic, CDD is associated with a range of behavioral abnormalities[16] that implicate pathology in different regions of the brain, suggesting that CDKL5 gene therapy must be distributed throughout the central nervous system (CNS) to be effective.

To determine the optimal route of administration, AAV9.Syn.hCDKL5 was administered to *Cdkl5* KO mice by either bilateral i.c.v. or a single unilateral i.c.m. injection at PND0 (study 1; Table 1). At approximately 5 weeks (35–37 days) post injection, tissues were collected and individual regions assessed for the presence of CDKL5 protein by electrochemiluminescence (ECL)-based immunoassay, h*CDKL5* mRNA by RT-qPCR, and vector genomes by qPCR. Doses are reported as vector genomes per gram of brain (vg/g). Overall, delivery of vector via i.c.v. resulted in more widespread and higher CDKL5 protein expression than i.c.m. delivery, except in the cerebellum (Figures 1A–1G). At the lowest tested i.c.v. dose, 3.6e11 vg/g, higher CDKL5 protein expression was seen in the olfactory bulb (96% of WT) and hippocampus (76% of WT), and lower levels in the striatum (35% of WT) and the cerebellum (41% of WT).

In addition to CDKL5 protein, we evaluated vector DNA and h*CDKL5* mRNA distribution (Figure S1). As shown in Figure 1H, levels of the vector genome correlated with the levels of h*CDKL5* mRNA (illustrated for i.c.v. injection, hippocampus tissue). No overt toxicity was noted at any dose.

AAV9.Syn.hCDKL5 restores phospho-EB2

To demonstrate that the CDKL5 protein expressed from the transgene has biological activity *in vivo*, we looked for its kinase activity. Microtubule-associated protein RP/EB family member 2 (end binding protein, EB2) is a microtubule plus-end tracking protein that is known to be phosphorylated by CDKL5.[17] In Cdkl5 KO mice, levels of phospho-EB2/total EB2 were 18% of those measured in WT mice. In mice administered increasing AAV9.Syn.hCDKL5 (study 1) by i.c.v. injection, phospho-EB2/total EB2 dose-dependently increased in tissues collected 5 weeks post dose. As shown in Figure 1I, CDKL5 protein and phospho-EB2/total EB2 increases were correlated (illustrated for the hippocampus). In vehicle-dosed Cdkl5 KO mice, levels of phospho-EB2/total EB2 were 19% of WT levels. At the lowest i.c.v. dose, 3.6e11 vg/g, levels of phospho-EB2 were 47% of WT levels, and CDKL5 protein levels were 76% of WT. At higher doses, levels of phospho-EB2 were normalized. Specifically, levels of phospho-EB2/total EB2 were 82% in mice dosed with 1.2e12 vg/g and CDKL5 protein levels were 210% of WT. At the highest i.c.v. dose, 3.6e12 vg/g, phospho-EB2/total EB2 levels were 112% of WT levels, and CDKL5 protein levels were 430% of WT levels.

Biodistribution measured by *in situ* hybridization

To further characterize biodistribution of AAV9.Syn.hCDKL5 11 weeks after i.c.v. or i.c.m. administration (study 1), we employed *in situ* hybridization (ISH) using a commercially developed RNAscope technique. Advanced Cell Diagnostics (ACD) developed specific probes for human CDKL5 mRNA, ensuring no cross-reactivity with murine *Cdkl5* mRNA. As depicted in Figure 2A, hCDKL5 mRNA delivered from AAV9.Syn.hCDKL5 was expressed in neurons as evidenced by its colocalization with a neuronal nuclei marker (NeuN protein). In contrast, h*CDKL5* mRNA did not colocalize with glial cells (Figure 2B) as demonstrated by the absence of co-expression of the glial cell marker glial fibrillary acidic protein (GFAP protein) and h*CDKL5*. This aligns with expectations, as the synapsin promoter is known to be specific for neurons.[18]

Please cite this article in press as: Voronin et al., Preclinical studies of gene replacement therapy for CDKL5 deficiency disorder, Molecular Therapy (2024), https://doi.org/10.1016/j.ymthe.2024.07.012

Table 1. Study summary and group designation for knockout mice

Study	Goal	Group	Mice	ROA	Dose, vg/g brain	*N*	Endpoints
1	Biodistribution and PD, male and female homozygous mice	1	*Cdkl5* KO	i.c.v.	vehicle	8	(1) vector DNA (5 weeks) (2) h*CDKL5* mRNA (5 weeks) (3) CDKL5 protein (5 weeks) (4) phospho-EB2 (5 weeks) (5) RNA ISH (11 weeks)
		2	*Cdkl5* KO	i.c.v.	3.60e11	8	
		3	*Cdkl5* KO	i.c.v.	1.20e12	8	
		4	*Cdkl5* KO	i.c.v.	3.60e12	8	
		5	*Cdkl5* KO	i.c.m.	vehicle	12	
		6	*Cdkl5* KO	i.c.m.	2.70e11	10	
		7	*Cdkl5* KO	i.c.m.	9.00e11	10	
		8	*Cdkl5* KO	i.c.m.	2.70e12	12	
		9	WT	–	–	8	
2	Dose response, male mice only	1	WT	i.c.v.	vehicle	29	(1) HLC (11 weeks) (2) OFT (15 weeks), FC (17 weeks) (3) Golgi staining (18 weeks) (4) RNA ISH (18 weeks) (5) CDKL5 protein (18 weeks)
		2	*Cdkl5* KO	i.c.v.	vehicle	25	
		3	*Cdkl5* KO	i.c.v.	3e9	27	
		4	*Cdkl5* KO	i.c.v.	3e10	23	
		5	Cdkl5 KO	i.c.v.	3e11	30	
3	Additional dose-response testing, male mice only	1	WT	i.c.v.	vehicle	24	(1) OFT (14 weeks) (2) FC (16 weeks) (3) ISH (19 weeks) (4) CDKL5 protein (19 weeks)
		2	*Cdkl5* KO	i.c.v.	vehicle	22	
		3	*Cdkl5* KO	i.c.v.	3e11	23	
		4	*Cdkl5* KO	i.c.v.	5e11	24	

Cdkl5, cyclin-dependent kinase-like 5 gene; FC, fear conditioning; HLC, hindlimb clasp; i.c.m., intra-cisterna magna; i.c.v., intracerebroventricular; ISH, *in situ* hybridization; KO, knockout; *N*, number evaluated; OFT, open-field test; PCR, polymerase chain reaction; PD, pharmacodynamics; ROA, route of administration; RT-qPCR, reverse transcription-quantitative polymerase chain reaction; WT, wild type.

Figure 2C compares the percentage of cells that are double-positive for h*CDKL5* mRNA and NeuN protein after i.c.v. or i.c.m. administration. Data are reported in ranges (1%–25%, 26%–50%, 51%–75%, 76%–100%) of NeuN (neuronal-specific marker)-h*CDKL5* double-positive cells. Areas throughout the entire brain (one hemisphere) were evaluated, and the mean percentage of hCDKL5/NeuN double-positive neuronal cells is reported. The percentage of double-positive cells increased with increasing dose when the gene therapy was administered by i.c.v. dosing. In contrast, no further increase in the percentage of total brain cells that were positive was seen with escalating i.c.m. dosing. The absence of global h*CDKL5* staining by ISH after i.c.m. dosing aligns with the limited expression of protein measured by ECL in similar brain regions. These data confirm that i.c.v. administration results in broader expression of h*CDKL5* than does i.c.m. delivery. At the lowest i.c.v. dose tested, 3.6e11 vg/g brain, overall h*CDKL5* staining of NeuN-positive cells fell within the lowest range (1%–25%). At 1.2e12 vg/g, the percentage of h*CDKL5*-NeuN double-positive cells was in an intermediate range (26%–50%), and at 3.6e12 vg/g the percentage of h*CDKL5*-NeuN double-positive cells was the highest (51%–75%).

Treatment of *Cdkl5* knockout mice with AAV9.Syn.hCDKL5 reduced hindlimb clasping at 3e11 vg/g

After identifying i.c.v. as the best route of administration, a second study was conducted to determine whether AAV9.Syn.hCDKL5 improves the phenotype of *Cdkl5* KO mice when dosed at PND0 by i.c.v. administration (study 2). Mice were dosed at 3e9, 3e10, and 3e11 vg/g brain. At 11 weeks post dose, the hindlimb clasp (HLC) response was assessed. When a mouse is lifted by the tail and then lowered toward a surface, a neurotypical mouse will extend all four limbs in anticipation of landing (an HLC score of 0). In contrast, a mouse with neurological deficit tends to pull its limbs toward the body to various degrees, resulting in an elevated HLC score (HLC score of 1, 2, or 3). As shown in Figure 3A, vehicle-dosed *Cdkl5* KO mice exhibited increased HLC scores relative to WT mice, consistent with published data.[9,15] Treatment with the two lower doses of AAV9.Syn.hCDKL5 failed to reduce HLC, but 3e11 vg/g completely prevented HLC and normalized the response to the test ($p < 0.001$).

Treatment of *Cdkl5* KO mice with AAV9.Syn.hCDKL5 reduced hyperactivity as measured with the open-field test at 5e11 vg/g

Cdkl5 KO mice have been reported to exhibit hyperactivity as measured by increased mobility in an open-field test (OFT).[15] As shown in Figure 3B, when placed into an open field, 15-week-old *Cdkl5* KO mice traveled a greater distance than did the WT mice, consistent with hyperactivity. Treatment with AAV9.Syn.hCDKL5 at 3e9, 3e10, or 3e11 vg/g did not reduce this hyperactivity (study 2; Table 1).

To define more precisely the dose-response relationship, an additional study (study 3: Table 1) was conducted to confirm these results, testing 3e11 vg/g and 5e11 vg/g. In study 3, although reaching statistical significance, less difference was seen in hyperactivity between

Please cite this article in press as: Voronin et al., Preclinical studies of gene replacement therapy for CDKL5 deficiency disorder, Molecular Therapy (2024), https://doi.org/10.1016/j.ymthe.2024.07.012

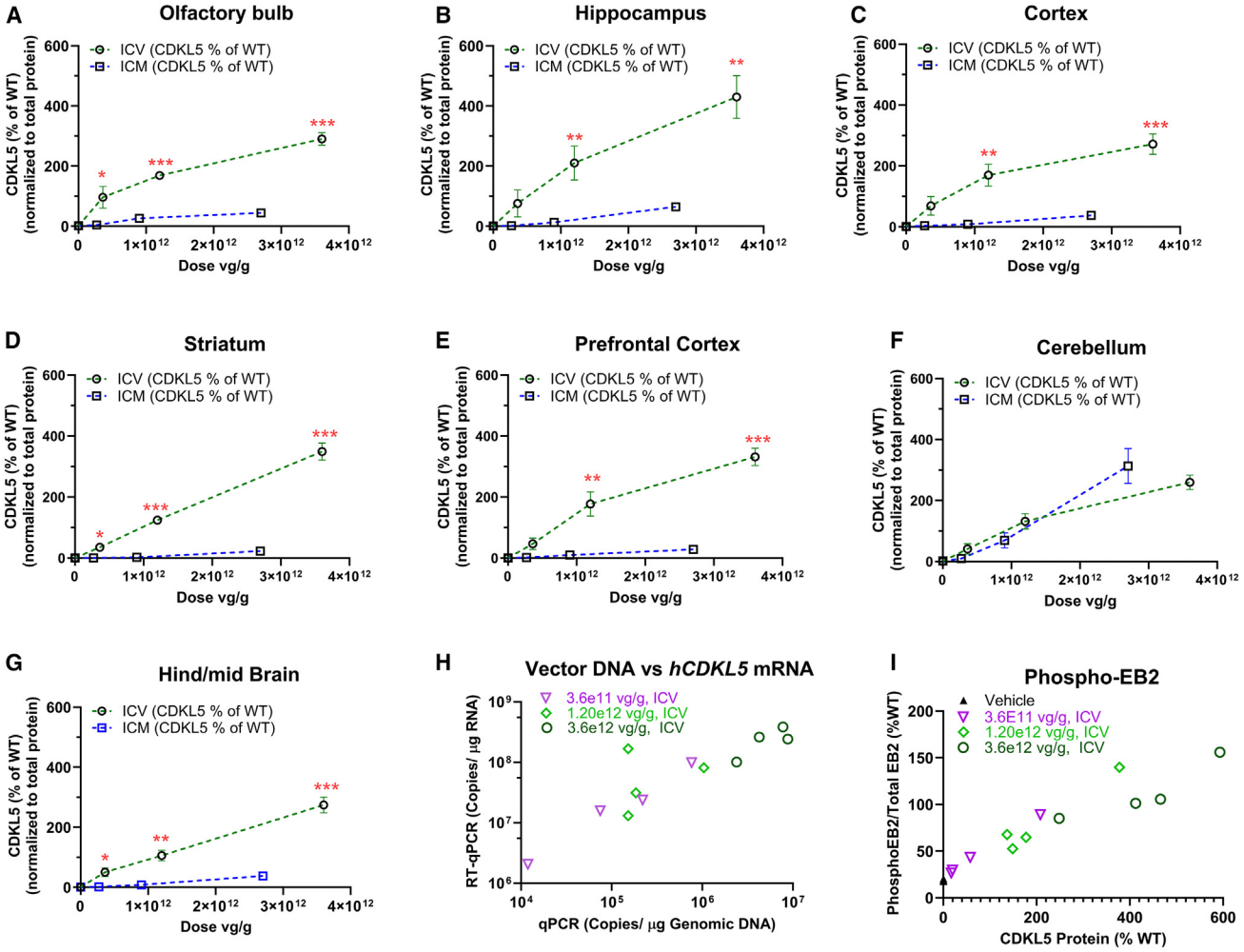

Figure 1. Increased biodistribution in Cdkl5 knockout mice after i.c.v. injection compared to i.c.m. injection at postnatal day 0

Symbols represent the mean ± SEM of 4 mice per group. (A–G) Comparison of biodistribution of CDKL5 protein levels in brain tissues 35–37 days after i.c.v. or i.c.m. administration of AAV9.Syn.hCDKL5 vector. (H) Correlation between vector DNA and gene expression, h*CDKL5* mRNA. Symbols represent DNA (qPCR) and RNA (RT-qPCR) values for individual animals. (I) Increases in phospho-EB2 with increasing CDKL5 protein levels in the hippocampus. Symbols in (H) and (I) represent individual animals. Dose is reported as vg/g brain weight. ***$p < 0.001$, **$p < 0.01$, *$p < 0.05$ (Student's t test comparing i.c.v. to comparable i.c.m. dose).

Cdkl5 KO and WT mice. As shown in Figure 3C, at 14 weeks of age hyperactivity was mitigated in mice dosed via i.c.v. delivery at 5e11 vg/g, although this difference (43% normalization, $p = 0.39$) did not reach significance due to the limited difference in hyperactivity. In study 3, because the difference in hyperactivity between the WT and *Cdkl5* KO mice was small, the time that the mice were specifically in the highly mobile state (as opposed to mobile or immobile) was also analyzed. As shown in Figure 3D, the time spent in the highly mobile state was reduced (46% reduction, $p < 0.01$) at a dose of 5e11 vg/g but not at a dose of 3e11 vg/g.

Treatment of *Cdkl5* knockout mice with AAV9.Syn.hCDKL5 reduced the fear-conditioning deficit at 5e11 vg/g

Learning and memory can be measured in rodents using the fear-conditioning assay. This test evaluates the ability of the mouse to learn and remember an association between a mild foot shock and a specific context. In the context of this assay, after being trained to associate specific context and cues with a shock, WT mice will typically freeze as a fear response after being challenged with the context and cues approximately 50% of the time.

Learning and memory in both study 2 and study 3 were measured using the fear-conditioning assay. As shown in Figure 3D. *Cdkl5* KO mice showed reduced freezing compared to WT mice after training, consistent with the published data.[19] In study 2 (at 17 weeks), as shown in Figure 3E, no significant improvement in the fear-conditioning response was observed in *Cdkl5* KO mice dosed at 3e9 vg/g or 3e10 vg/g, but recovery at 3e11 vg/g reached statistical significance (44%, $p < 0.05$). In study 3 (at 16 weeks), as shown in Figure 3F, improvement was seen at 3e11 vg/g (62%, though not reaching

Please cite this article in press as: Voronin et al., Preclinical studies of gene replacement therapy for CDKL5 deficiency disorder, Molecular Therapy (2024), https://doi.org/10.1016/j.ymthe.2024.07.012

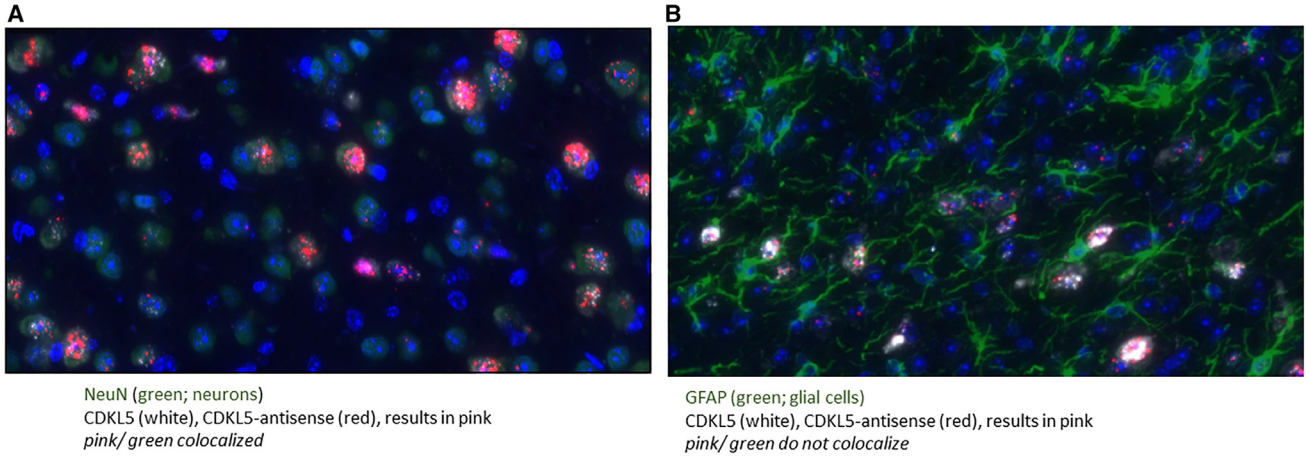

C

	ICV, *Cdkl5* KO				ICM, *Cdkl5* KO				WT
Dose vg/g brain	**0**	**3.6e11**	**1.2e12**	**3.6e12**	**0**	**2.7e11**	**9e11**	**2.7e12**	**0**
Percent double positive	0	1-25	26-50	51-75	0	1-25	1-25	1-25	0

Figure 2. Expression of hCDKL5 mRNA in neurons but not glial cells after administration of AAV9.Syn.hCDKL5 at postnatal day 0

Three mice per group were evaluated. Images of the cortex are shown at 40× magnification. (A) Expression of h*CDKL5* (pink) mRNA in NeuN protein positive neurons (green) after i.c.v. administration at 3.6e11 vg/g. (B) Lack of expression of h*CDKL5* mRNA (pink) in glial fibrillary acidic protein (GFAP)-positive glial cells (green). (C) Comparison of distribution after i.c.v. or i.c.m. administration. Shown are the percentage of cells in the hemisphere that are double-positive for h*CDKL5* mRNA and for NeuN. The probes are selective for human *CDKL5* mRNA and do not cross-react with murine *Cdkl5* mRNA. Regions across the entire brain were evaluated.

statistical significance), and complete normalization was seen at 5e11 vg/g ($p < 0.01$).

Treatment of *Cdkl5* knockout mice with AAV9.Syn.hCDKL5 improved the dendritic morphology at doses of 3e10 and 3e11 vg/g

The morphological features of pyramidal cells in the CA1 hippocampal subfield were quantified in study 2 animals that were approximately 18 weeks old following Golgi-Cox staining. Pyramidal neurons contain two types of dendrites (basal and apical). Several characteristics of these dendrites were analyzed. Representative images of CA1 hippocampal pyramidal cells from the different treatment groups are shown in Figure 4A. Consistent with published data, CA1 pyramidal neurons of *Cdkl5* KO mice display significant differences in dendritic morphology compared to that of the WT control group (Figures 4A and S2), including reduced dendritic lengths (Figure 4B), spine counts (Figure 4C), and overall spine densities (Figure S2).[9,19] Furthermore, significant reductions in dendritic ramifications (arborizations or the branching out of dendrites that allow for potential synaptic connections), depending on the distance from the soma of the pyramidal cell, were observed in the neurons of *Cdkl5* KO mice compared to vehicle-dosed WT mice (Figure S2).

Following treatment with AAV9.Syn.hCDKL5, significant dose-dependent increases in dendritic lengths, spine counts, spine density, and dendritic ramifications were observed, reaching statistical significance at 3e10 vg/g and with near-normalization at 3e11 vg/g. As shown in Figures 4B and 4C, when quantified, improvements were seen at a dose of 3e10 vg/g (reaching statistical significance), and the effect was more pronounced at a dose of 3e11 vg/g.

Correlation of biodistribution and expression with behavior

The initial biodistribution and tolerability study (study 1) examined distribution after delivery of doses of 3.6e11, 1.2e12, and 3.6e12 vg/g of AAV9.Syn.hCDKL5. Subsequent studies (study 2 and study 3) focused on efficacy. However, CDKL5 protein expression levels and h*CDKL5* mRNA/ISH were also analyzed in these efficacy studies (studies 2 and 3). Results for protein and h*CDKL5* mRNA/ISH are summarized in Table 2. Additional details on protein expression are included in Figure S3 and Table S1. Animals from study 2 (3e9, 3e10, and 3e11 vg/g) and study 3 (3e11 and 5e11 vg/g) were euthanized at approximately 18 and 17 weeks old, respectively. Table 2 (4^{th} column, RNAscope data) summarizes both the staining score of h*CDKL5* mRNA (number of dots per cell) and the percentage of NeuN protein (a neuronal marker) staining for h*CDKL5* mRNA. For the staining score, a semi-quantitative score of 0–4 was utilized. For the percentage of double-positive staining cells, ranges are reported.

Levels of (murine) CDKL5 protein were minimal (<2% of WT) in the male *Cdkl5* KO mouse, whereas CDKL5 protein increased with increasing AAV9.Syn.hCDKL5 dose. Less increase in CDKL5 protein

Please cite this article in press as: Voronin et al., Preclinical studies of gene replacement therapy for CDKL5 deficiency disorder, Molecular Therapy (2024), https://doi.org/10.1016/j.ymthe.2024.07.012

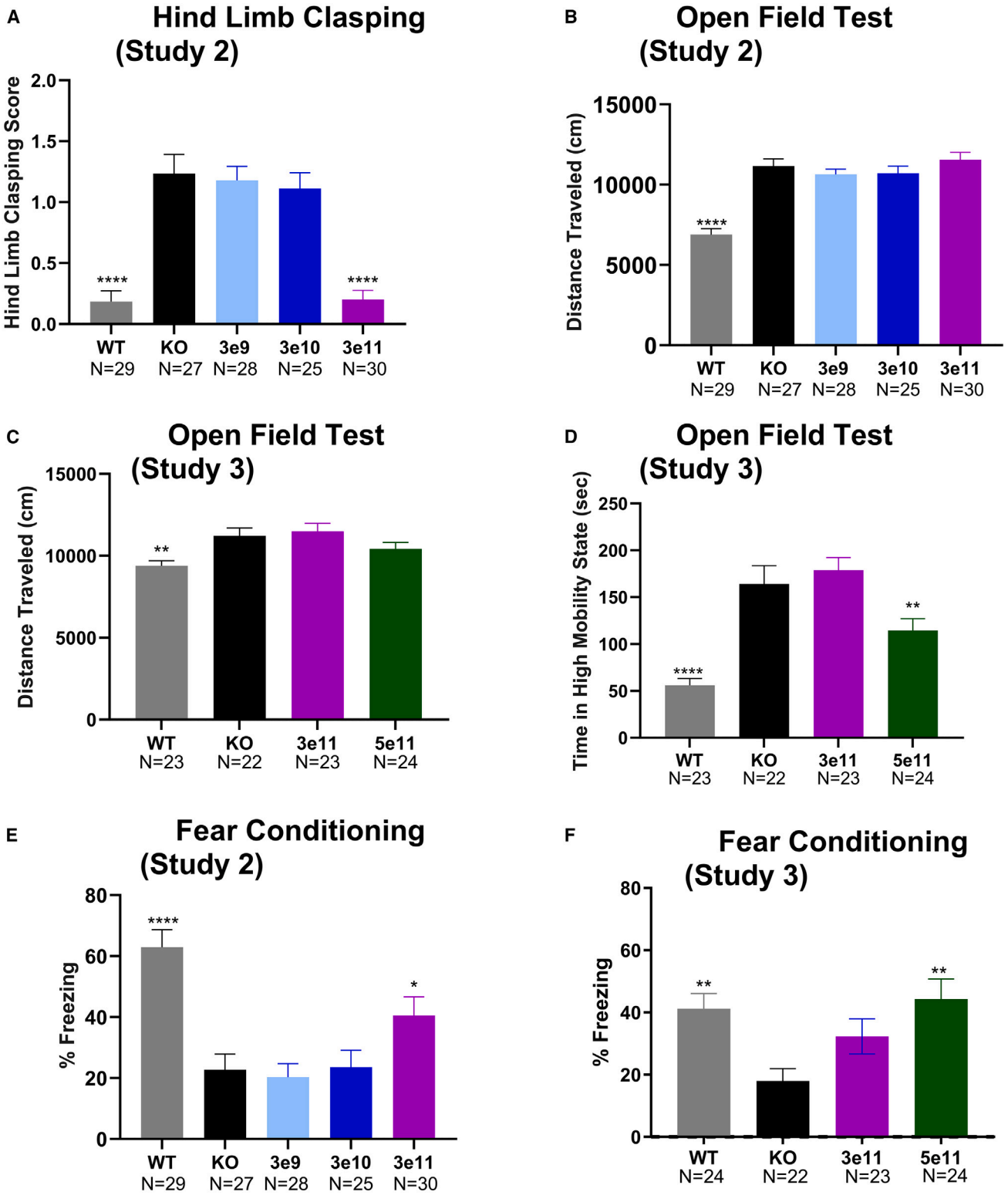

(legend on next page)

Please cite this article in press as: Voronin et al., Preclinical studies of gene replacement therapy for CDKL5 deficiency disorder, Molecular Therapy (2024), https://doi.org/10.1016/j.ymthe.2024.07.012

levels was seen in the cerebellum than in the hippocampus or the cortex. At 3e9 vg/g or 3e10 vg/g, levels of CDKL5 protein were low, aligning with the observed lack of efficacy. ISH specifically recognized human *CDKL5* mRNA. Human *CDKL5* mRNA expression based on the percentage of NeuN-hCDKL5 double-positive neurons increased with increasing gene therapy dose. At lower doses, 3e9 and 3e10 vg/g, the percentage of cells staining double-positive was low, in the range of 1%–10%. At a dose of 3e9 and 3e10 vg/g, the staining score (dots per cell) was 2–3 and 3–4, respectively. Consistent with the limited h*CDKL5* mRNA expression at these doses, measurable but limited improvement was noted in the functional tests.

At a dose of 3e11 vg/g i.c.v., CDKL5 protein expression reached measurable levels with average values from the two studies of 14%, 78%, and 61% of WT mice in the cerebellum, hippocampus, and cortex, respectively. Moreover, the percentage of cells staining double-positive was higher than with the lower doses. At this dose, improvements in Golgi staining, fear conditioning, and HLC were measured, although hyperactivity was not reduced. At the higher dose of 5e11 vg/g, the hyperactivity (as measured by OFT) was reduced and protein expression was increased relative to that measured at a dose of 3e11 vg/g in all three tissues. Biodistribution showed that a greater percentage of cells were double-positive at 5e11 vg/g.

Biodistribution and tolerability in the nonhuman primate

Biodistribution and tolerability of AAV9.Syn.hCDKL5 by i.c.v. administration was assessed in a non-GLP (good laboratory practices) study of cynomolgus monkeys (Table 3). Three different groups were dosed with AAV9.Syn.hCDKL5. Two groups were dosed unilaterally with 2e10 vg/g (equivalent to 1.5e12 vg/monkey) and 2e11 vg/g (equivalent to 1.5e13 vg/monkey). The third group was dosed bilaterally with a 2e11 vg/g total. No AAV9.Syn.hCDKL5-related mortality occurred; all animals survived to the scheduled euthanasia at 4 weeks post dose. No AAV9.Syn.hCDKL5-related clinical or neurological observations were noted, as well as no effects on body weight (Table S2) and no changes in hematology (Table S3), coagulation (Table S4), or clinical chemistry (Table S5). As shown in Figure 5A, broad biodistribution was seen with measurable transduction throughout the brain and dose-dependent increases comparing the lower dose to the higher dose. The lowest distribution was to the putamen. Samples were not obtained from the cerebellum or hindbrain. There were no overt differences in the biodistribution when the therapy was administered unilaterally relative to bilateral administration. As shown in Figure 5B, significant exposure was seen in the peripheral organs, particularly in the liver.

DISCUSSION

While many rare neurodevelopmental disorders currently have no effective treatments, developing gene replacement therapies for monogenic disorders like CDD is a promising avenue of research. We have shown the potential of i.c.v. delivery of gene therapy replacement employing AAV9.Syn.hCDKL5 as a treatment for CDD. We demonstrate both biodistribution and efficacy in a mouse model of CDD as well as biodistribution and tolerability in NHPs. These data demonstrate that i.c.v. delivery provides broader biodistribution than does i.c.m. delivery in mice when injected at PND0. In the context of CDD where the pathology involves multiple regions of the brain, achieving broad distribution throughout the entire brain is necessary. Conversely, for some CNS diseases where the cerebellum is the primary target, i.c.m. dosing may be preferable. Few nonclinical rodent studies have provided a side-by-side comparison of i.c.v. and. i.c.m. gene therapy for neurodevelopmental disorders. While several studies have demonstrated effective biodistribution published using i.c.m. delivery, these studies did not include a side-by-side comparison with i.c.v. administration.[20,21] The evaluation of the extent of biodistribution will depend on the sensitivity of the detection assay, making comparisons across models and investigational laboratories challenging. Our studies also indicate that in the NHPs, similar biodistribution was seen with unilateral and bilateral administration.

Other publications have assessed the efficacy of CDKL5 gene therapy using *Cdkl5* KO mice, PHP.B capsid, nonselective promoter, and i.v. dosing. We utilized a neuronal-specific promoter and i.c.v. dosing. Consistent with previous reports, the synapsin promoter provided high, selective neuronal expression of the target gene.[22] Gao et al. evaluated efficacy of AAV-PHP-B-based CDKL5 gene therapy after i.v. dosing of 1-month-old mice, using the PHP-B capsid,[13] which is known to have very good transport into the CNS in some strains of mice but not in NHPs. Both glial and neuronal cells were transfected. They reported a partial reduction in the HLC phenotype, modest improvement in the rotarod assay, and some reduction in the hyperactivity as measured by the OFT. At a dose of 3e11 vg/g i.c.v., we report near-complete normalization of the HLC but no effect on hyperactivity as measured in the OFT. At 5e11 vg/g, we see about 43% reduction in hyperactivity as measured with the OFT. In the paper by Gao et al., they did not observe sufficient freezing in the fear-conditioning assay with the WT mice to have a sufficient window to measure efficacy, limiting comparison to what we report.[13] Only a single concentration of vector was assessed by Gao's group but, comparable to the data reported here, about

Figure 3. AAV9.Syn.hCDKL5 improved behavior of Cdkl5 KO mice

(A) Hindlimb clasp measured at 11 weeks of age. Bars represent the mean score ± SEM (study 2). (B) Open-field distance traveled (cm) (study 2) measured at 15 weeks. (C) Open-field distance traveled (cm) (study 3) measured at 14 weeks. (D) Open-field highly mobile state (study 3) measured at 14 weeks. (E) Fear conditioning post training percent freezing (study 2) measured at 17 weeks. (F) Fear conditioning (higher doses) post training percent freezing (study 3) measured at 16 weeks. Dose values on x axis are in vg/g brain delivered i.c.v. Number per group is shown below the x axis. Statistics show comparison to *Cdkl5* KO vehicle-dosed mice evaluated by a one-way ANOVA followed by Dunnett's multiple comparison test ($p \leq 0.05$) where $^{****}p < 0.0001$, $^{***}p \leq 0.001$, $^{**}p \leq 0.01$, and $^{*}p \leq 0.05$.

Please cite this article in press as: Voronin et al., Preclinical studies of gene replacement therapy for CDKL5 deficiency disorder, Molecular Therapy (2024), https://doi.org/10.1016/j.ymthe.2024.07.012

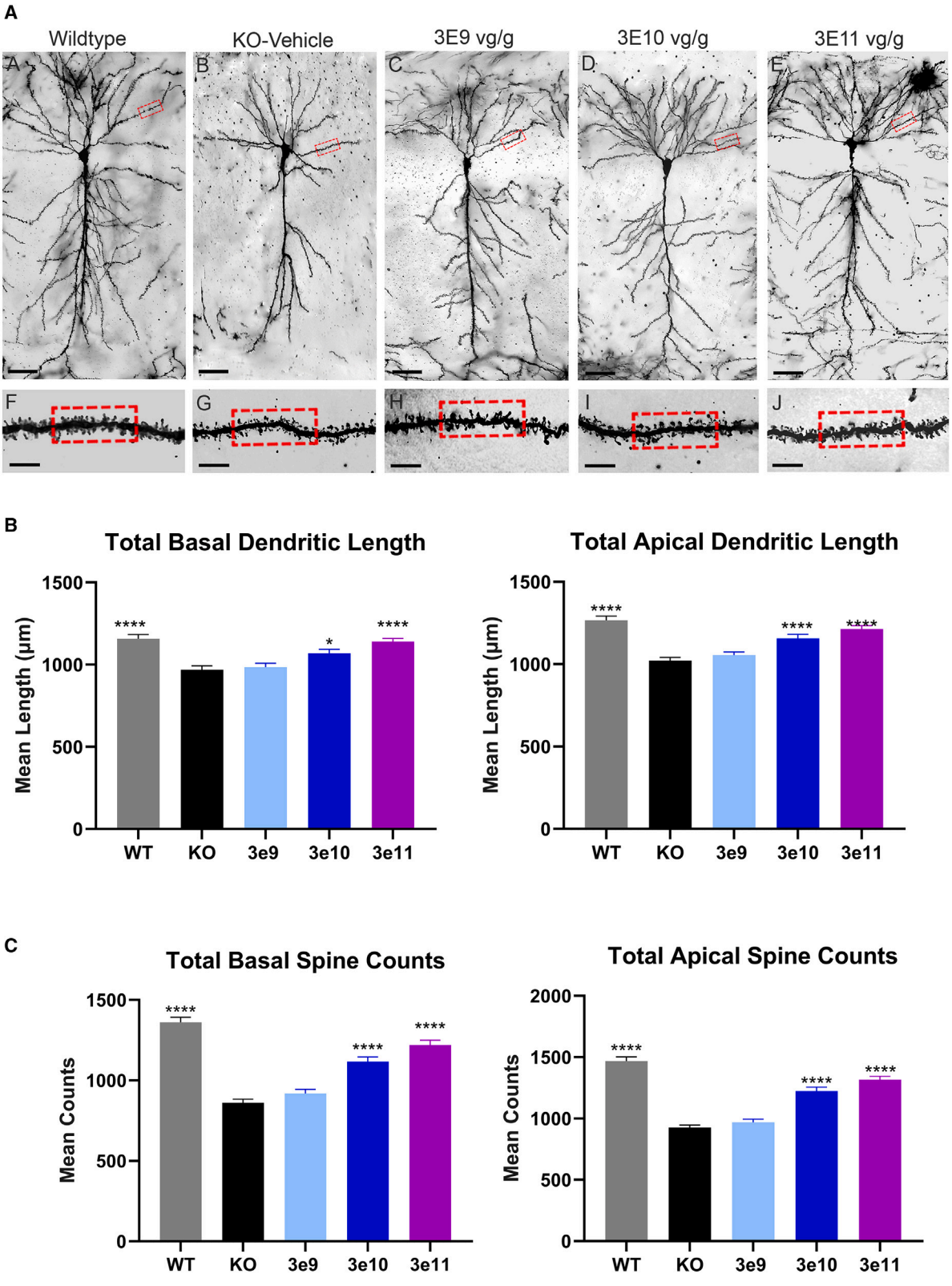

(legend on next page)

Please cite this article in press as: Voronin et al., Preclinical studies of gene replacement therapy for CDKL5 deficiency disorder, Molecular Therapy (2024), https://doi.org/10.1016/j.ymthe.2024.07.012

Table 2. Summary comparing expression levels with functional improvements

		CDKL5 protein % wild type (mean ± SEM)			RNAscope: (1) score; (2) % of cells with NeuN/hCKDL5	Improvement shown in functional tests			
						Golgi staining	Fear conditioning	Open-field test	Hindlimb clasp
Dose vg/g brain	Study	HPC	Cortex	Cerebellum	Biodistribution	Dendritic morphology	Memory and learning	Hyperactivity	Neurological health
Vehicle	1, 2, 3	>1.5	>1.5	>1.5	0; 0 (3/3)	ND	ND	ND	ND
3.0e9	2	1.8 ± 0.3	1.3 ± 0.2	1.0 ± 0.2	2–3; <1 (2/3), 1–10 (1/3)	partial (10%***)	none	none	none
3.0e10	2	3.9 ± 1.0	2.2 ± 0.6	0.9 ± 0.2	3–4; 1–10 (3/3)	improved (54%****)	none	none	partial but not significant (12%)
3.0e11	2	33 ± 12	30 ± 14	10 ± 2	3–4; 11–25 (3/3)	improved (72%****)	improved (44%*)	none	improved (98%****)
3.0e11	3	123 ± 32	73 ± 22	18 ± 5	3–4; 26–50 (3/3)	ND	improved (62%) but not significant	partial but not significant (25%)	improved (100%), but genotype difference did not reach significance
5e11	3	347 ± 98	136 ± 21	33 ± 9	3–4; 26–50 (3/3)	ND	normalized (100%****)	improved (43%**)	improved (89%), but genotype difference did not reach significance

ANOVA, analysis of variance; CDKL5, cyclin-dependent kinase-like 5; HLC, hindlimb clasp; HPC, hippocampus; KO, knockout; NeuN, neuronal nuclei; SEM, standard error of mean; vg, vector genomes; None, no improvement; ND, no data.
Golgi-Cox staining values represent the average of the percent normalization for basal dendritic length, apical dendritic length, basal spine counts, and apical spine counts.
Protein expression is shown relative to wild-type levels.
Statistical analysis by ANOVA, multiple comparisons vs. vehicle-dosed *Cdkl5* KO: $^{*}p < 0.05$, $^{**}p < 0.01$, $^{***}p < 0.001$, $^{****}p < 0.0001$.

50% of the brain area expressed the vector with the i.v. dose administered.[13]

Medici et al., utilizing an AAVPHP.B-based capsid delivered i.v., showed limited activity in adult mice.[15] This contrasts with the study by Gao et al., where i.c.v. delivery of AAV9.Syn.hCDKL5 at PND0 was reported to be more effective when compared in the same assays (hyperactivity/OFT and Golgi-Cox staining) than AAVPHP.B delivered i.v. to 3-month adult mice.[13] Efficacy reported with the i.v. delivery of CDKL5-IgkTAT that results in secreted TAT-CDKL5 protein was similar to what we report with i.c.v. delivery of AAV9.Syn.hCDKL5. Medici et al. utilized i.c.v. injection of neonatal mice to evaluate biodistribution and i.v. dosing to evaluate efficacy, so we cannot correlate biodistribution of their vector with efficacy.[15]

Published data suggest that CDKL5 plays a crucial role not only in neurodevelopment but also in neuronal maintenance.[23,24] Using genetic manipulation, *Cdkl5* was deleted from adult mice, which showed CDD-like symptoms.[23] More importantly from a therapeutic perspective, genetic restoration of *Cdkl5* in adult mice resulted in a reduction in pathology. Our studies did not assess the optimal temporal window for gene therapy but rather focused on the dose response. We dosed at PND0 to maximize biodistribution in the rodent and with subsequent validation in the NHP model. There were no evident signs of toxicity in the NHP study.

Evaluation of biodistribution at 11 weeks post dose following i.c.v. injection at PND0 showed that up to 75% of neurons can be transfected. Notably, glial cells were not transfected. This suggests that despite subsequent increases in brain size, most neurons present at PND0 were present in adults. The neurons that did not have vector DNA at the high dose (25%) likely were not transfected at PND0, although they potentially could have been formed after PND0. This result aligns with existing literature, which indicates that the surge in rodent brain size during the initial 3 weeks of life primarily involves an increase in glial cells rather than neurons.[25]

Our study utilizing i.c.v. dosing, as well as the earlier studies from other laboratories, supports the hypothesis that delivery of CDKL5 by gene therapy should benefit patients with CDD. Here, we further characterize this by assessing the dose response. Notably, significant correction of CDD-like phenotypes was seen at doses of 3e11 to 5e11 vg/g, with limited or no correction at lower doses. Evaluated phenotypes in this study included HLC, OFTs, fear

Figure 4. Dendritic morphology is improved after treatment with AAV9.Syn.hCDKL5
(A) Normalization of dendritic morphology. Representative images of CA1 hippocampal pyramidal cells across groups. Compared to WT mice, *Cdkl5* KO mice exhibited significant reductions in dendritic morphology (upper panel; scale bar, 50 μm) as well as the spines of CA1 pyramidal basal dendrites (box in the lower panel; scale bar, 5 μm). (B and C) Bars show the mean ± SEM (8 mice/group) for basal and apical pyramidal cell dendritic length (B) and spine count (C). Dose values on the x axis are in vg/g brain. Statistics show comparison to *Cdkl5* KO vehicle-dosed mice evaluated by a one-way ANOVA followed by Dunnett's multiple comparison test ($p \leq 0.05$) where $^{****}p < 0.0001$, $^{***}p \leq 0.001$, $^{**}p \leq 0.01$, and $^{*}p \leq 0.05$.

Please cite this article in press as: Voronin et al., Preclinical studies of gene replacement therapy for CDKL5 deficiency disorder, Molecular Therapy (2024), https://doi.org/10.1016/j.ymthe.2024.07.012

Table 3. Group designation for nonhuman primate non-GLP biodistribution study

Group	Dose vg/animal	Dose vg/g brain	Injection	*N* (males)
1	1.5e12/animal	2.00e10	unilateral	3
2	1.5e13/animal	2.00e11	unilateral	3
3	1.5e13/animal	2.00e11	bilateral	3

Brain weights of 75 g were used to convert from dose (vg/animal) to dose (vg/g brain). *N*, number evaluated; vg, vector genomes.

conditioning, and CA1 hippocampal pyramidal neuron morphology by Golgi-Cox staining. The HLC test serves as a general indicator of neuronal health, as multiple areas of the brain have been implicated in this response, including the cerebellum and the striatum.[26] Hyperactivity was evaluated with the OFT. CDD in mice has been associated with a hyperactive phenotype as measured using the OFT. Learning and memory were evaluated using the fear-conditioning assay, acknowledging that the fear-conditioning test could be confounded by hyperactivity. Golgi staining demonstrated a normalization of the synaptic architecture. A deficit in the synaptic architecture would be consistent with reduced plasticity and, therefore, could lead to reduced ability for learning and memory. Different phenotypes were improved at different doses, but no improvements were seen at a dose of 3e9 vg/g brain. Consistent with the lack of efficacy, CDKL5 protein levels in *Cdkl5* KO mice at this dose were less than 2% of WT, and no h*CDKL5* mRNA signal was detected with ISH. At a dose of 3e10 vg/g, there was a modest improvement in the HLC (not reaching significance), but dendritic morphology was improved (reaching significance). However, open-field (hyperactivity) or fear-conditioning (learning and memory) tests were not improved with a dose of 3e10 vg/g. At this dose, CDKL5 protein levels were less than 4% of WT, and there was limited but measurable staining of h*CDKL5* mRNA with ISH (1%–10% of cells, the lowest range). At 3e11 vg/g, the fear-conditioning response was improved, but there was no reduction in hyperactivity. At this dose, h*CDKL5* mRNA and CDKL5 protein levels were higher. At 5e11 vg/g, the fear-conditioning response and hyperactivity were reduced. At 5e11 vg/g, h*CDKL5* mRNA and CDKL5 protein levels were increased above those measured at 3e11 vg/g.

Unlike *MECP2* or *UBE3A*, where gene duplication has been definitively associated with neurodevelopmental disorders MECP2 duplication syndrome (OMIM 300260)[27] and Dup15q syndrome (OMIM 608636),[28] respectively, an increase in CDKL5 copy number has not been clearly shown to be associated with genetic disorders. There is a publication showing CDKL5 duplications that are of regions less than 1 Mb, and the seven patients described showed a phenotype (albeit distinct and less severe than CDD).[29] Further, there is a single report of a gain-of-function mutation.[30] However, neither of these publications definitively show that overexpression of WT CDKL5 would be detrimental. Potentially, GLP toxicology studies may provide additional insight into the potential for overdosing CDKL5 before clinical studies are initiated. We include the non-GLP NHP study as evidence of tolerability. In our studies, we did not see any evidence of overt toxicity in mice or the NHPs, even at the highest doses of gene therapy delivered (3.6e12 vg/g mouse brain in study 1).

A key finding in our study is that broad biodistribution of the gene therapy vector is required to achieve activity. To achieve this broad biodistribution, a high dose is required. For clinical studies, a next generation vector using a capsid with higher biodistribution and lower titer may be preferable. There are several different strategies that could be used to enhance this vector. It is possible that administering this gene therapy with multiple routes of administration such as both i.c.v. and i.c.m. injection may result in broader biodistribution with lower titer. Because *CDKL5* mRNA expression is highest in neurons, we chose to utilize the synapsin neuronal-specific promoter. Nonetheless, low expression of CDKL5 mRNA is reported in glial cells in mice[13] and cultured rat glial cells,[31] although no published autonomous deficits in these cells have been reported. It is possible that a therapeutic that delivered both isoform 1 and isoform 2 or a nonselective promoter may be more beneficial. Additional preclinical studies would be necessary to confirm whether any of these approaches reduced the required dose or improved efficacy.

Because of the limitations in current gene therapy technology, the extent of CDKL5 gene replacement with the vector described here may not be complete. However, the correction of the molecular architecture as shown by the Golgi-Cox staining, even at doses where there is no overt improvement in functional behavior, is encouraging.

These current studies are limited by using only male *Cdkl5* KO mice. Subsequent studies could evaluate the dose response in female mice. Further, we did not evaluate the reversibility of all aspects of the disease such as autistic behaviors or seizures, which are important components of the human disease. Subsequent studies could evaluate the dose response for endpoints that would evaluate these phenotypes. Additionally, the doses administered in the NHP study were lower than the highest doses used in the mouse studies and, therefore, additional studies are needed to evaluate safety.

In summary, the data reported here show that i.c.v. delivery of the human CDKL5 gene holds potential to provide clinical benefit in human CDD. Further, these data have broader implications in the treatment of other CNS diseases with gene therapy.

MATERIALS AND METHODS

Cloning, production, and titer determination of AAV vectors

AAV9.Syn.hCDKL5 is composed of a single-stranded codon-optimized complementary deoxyribonucleic acid (cDNA) containing adeno-associated virus serotype 2 (AAV2) inverted terminal repeats, the human CDKL5 gene driven by a synapsin promoter, and bovine growth hormone polyadenylation (bGH pA) signal. Vector was

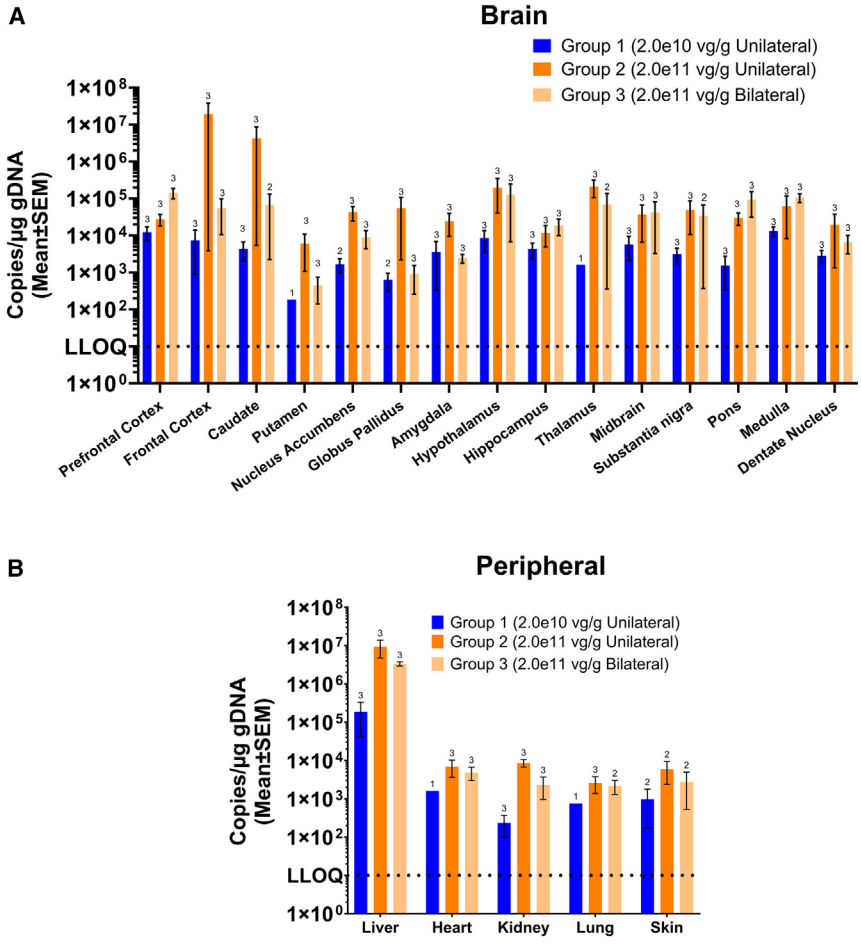

Figure 5. Biodistribution of AAV9.Syn.hCDKL5 in nonhuman primates

AAV9.hSyn.CDKL5 vector after i.c.v. administration is detectable throughout the brain (A) and periphery (B) in nonhuman primates. Values represent the mean ± SEM. The number above the bar represents the number of animals for which data were available for that tissue. Biodistribution of vector measured in the CNS using qPCR.

produced and purified as described in supplemental information. As summarized in Figures S4, S5, and Table S6, the quality control analysis demonstrated that the test material contained approximately 15% empty capsids. Capsids were evaluated by polyacrylamide gel electrophoresis and were stained using ProteoSilver silver staining (Sigma), while genome integrity was evaluated by alkaline gel analysis and nanopore DNA sequencing.

Quantitative bioassays

Genomic DNA was isolated with QIAcube HT (Qiagen #80204) according to the manufacturer's instructions. Total RNA was isolated using QIAcube automation and a customized protocol for tissue using the RNeasy 96 QIAcube HT Kit.

Tissues for protein analysis were homogenized using the TissueLyser II system (Qiagen, Germantown, MD) in a homogenization buffer (50 mM Tris-HCl [pH 7.5], 300 mM NaCl, 1 mM $MgCl_2$, 3 mM EDTA, 1% Triton X-100, 10% glycerol) containing a cocktail of protease and phosphatase inhibitors at 100 mg tissue per mL of buffer. The homogenates were centrifuged to remove insoluble protein and other debris, and the supernatants were divided into aliquots in triplicate multiwell microplates. Total protein was quantified using the bicinchoninic acid (BCA) protein assay.

CDKL5 DNA assay using qPCR

Forward primer hCDKL5_F-5: 5′ TGA GCA GCT GGG AGC AAA GT 3′

Reverse primer hCDKL5_R-5: 5′ CAT CCT GCT TCT ATT GGT CCT GTT 3′

hCDKL5_Probe-5: 5′ 6FAM-CGG ACC TAA CGG ACA CC-MGBNFQ 3′

Linearized pAAV.hSyn-hCDKL5_1_optimized for human-WPRE plasmid was used as a standard. The linearized DNA was purified using the QIAquick PCR purification kit (Qiagen, #28104) according to the manufacturer's instructions. The concentration and purity of the linearized plasmid were determined using Cytation 5 (Biotek) and Take3/Take3 Trio. Complete digestion of the plasmid was confirmed by agarose gel electrophoresis. Copy number of the linearized plasmid per µL was determined according to the equation

$$\text{Number of copies} = \frac{[\boldsymbol{X}\ \text{ng} \times 6.022 \times 10^{23}\text{molecules/mole}]}{[\boldsymbol{N}\ \text{bp} \times 650\text{g/mole} \times 1 \times 10^{9}\text{ng/g}]},$$

where $\boldsymbol{X}$ is amount of double-stranded DNA (dsDNA) (ng) and $\boldsymbol{N}$ is length of dsDNA (bp).

A dilution of the genomic DNA in a DNA LoBind plate to a concentration of 50 ng/µL with nuclease-free water was made. A standard curve was generated using 10-fold serial dilutions of the linearized standard plasmid in DNA LoBind Tubes to generate a standard curve. A total of 16 µL of the master mix (containing PerfeCTa qPCR ToughMix uracil *N*-glycosylase (UNG), 0.3 µM forward primer, 0.9 µM reverse primer, 0.25 µM probe, and TaqMan Copy Number Reference Assay, mouse, Tfrc, VIC-MGB) were added to each well of the MicroAmp EnduraPlate optical 384-well clear reaction plate. A volume of 4 µL of the diluted genomic DNA samples (50 ng/µL), standard plasmid (eight concentrations ranging from 2.5e+0 to 2.5e+7 copy number/µL), or nuclease-free water (NTC) was added to the wells and the plate sealed with a MicroAmp optical adhesive

film. The plate was run in a Bio-Rad CFX384 system using the following PCR cycle conditions. An initial UNG incubation was carried out for 5 min at 45°C, followed by a denaturation reaction for 7 min at 95°C. Subsequently, 40 cycles of PCR that included 15 s at 95°C and 1 min at 60°C per cycle was conducted and the plates read. The data were analyzed using Bio-Rad CFX manager software.

CDKL5 mRNA assay using RT-qPCR

Human CDKL5 synthetic RNA (transcript 4; IDT #17508277; ref. #296408196) was used as a standard. A volume of 16 μL of the master mix (containing qScript XLT 1-Step RT-qPCR ToughMix, Low ROX, 0.1 μM forward primer, 0.6 μM reverse primer, 0.25 μM probe, and TaqMan Copy Number Reference Assay, mouse, Tfrc, VIC-MGB) was added to each well of the MicroAmp EnduraPlate optical 384-well clear reaction plate. A volume of 4 μL of the diluted RNA samples (25 ng/μL), standard (seven concentrations ranging 2.5e+1 to 2.5e+7 copy number/μL), or NTC was added to the wells, and plates were sealed with a MicroAmp optical adhesive film. Each plate was run in the QuantStudio 7Pro system using the following cycle conditions. cDNA synthesis was initiated by incubation at 50°C for 10 min followed by denaturation for 1 min at 95°C. Subsequently, 40 cycles of PCR that included 15 s at 95°C and 1 min at 60°C per cycle was conducted and the plates read. The data analysis was carried out using Design & Analysis 2.3 (DA2.3) software.

CDKL5 protein assay using and electrochemiluminescence-based immunoassay

Protein levels of CDKL5 in brain tissues from the olfactory bulb, prefrontal cortex, striatum, hippocampus, motor/parietal cortex, cerebellum, and midbrain/brainstem were measured using an ECL CDKL5 assay on the Meso Scale Discovery (MSD) platform. CDKL5 antibodies used in the capture and detection positions were EMD Millipore anti-CDKL5 antibody (MABS1132) and Invitrogen anti-CDKL5 antibody (PA5-19506), respectively. Sulfo-tagged goat anti-rabbit secondary detection antibody (MSD R32AB-5) was used. All tissue samples were diluted to a final total protein concentration of approximately 500 μg/mL. The quantity of CDKL5 protein for each sample was represented as the ECL signal divided by the total protein. The CDKL5 protein levels for the *Cdkl5* KO and treated mice were then represented as the percentage of CDKL5 levels present in the WT mice.

In situ hybridization

A RNAscope *in situ* hybridization assay (RNAscope 2.5 LS RED ISH) was developed and performed by ACD (Newark, CA). Brains were collected and sagittal sections evaluated. Semi-quantitative visual scoring was performed at 40× magnification. Scores were based on the number of fluorescent dots per cell and were quantified visually. Data were reported as both the staining score and the percentage of positive cells. The staining score was reported as 0–4 (gene expression level). A score of 0 corresponds to no staining or <1 dot/10 cells; a score of 1 corresponds to 1–3 dots/cell; a score of 2 corresponds to 4–9 dots/cell with no or very few dot clusters; a score of 3 corresponds to 10–15 dots/cell and/or <10% dots are in clusters; and a score of 4 corresponds to >15 dots/cell and/or >10% dots are in clusters. The percentage of positive cells was reported as cells double-positive for NeuN protein and h*CDKL5* mRNA. Percentage of cells positive was scored visually based on number of cells with >1 dot/cell and binned into categories. For study 1, cells with ≥ 1 dot per cell were considered positive, and percentage of cells positive were binned into categories (i.e., 0%, 1%–25%, 26%–50%, 51%–75%, or 76%–100%). For studies 2 and 3, categories were 0%, 1%–10%, 11%–25%, 26%–50%, 51%–75%, or 76%–100%.

Phospho-EB2/total EB2 ratio

Phospho-EB2 and total EB2 were measured using the western blotting method. Protein lysates for SDS-PAGE gel were prepared using Laemmli buffer to a final concentration of 1–2 mg/mL total protein. A total of 10 μg of protein was loaded onto 4%–20% Criterion Tris-HCl gel and transferred onto nitrocellulose membrane using a Bio-Rad *Trans*-blot Turbo Blotting system. The nitrocellulose was then probed with rabbit polyclonal anti-pS222 EB2 (Covalab, #pab01032-P) at 1 μg/mL and goat anti-rabbit IRDye 800CW (Li-cor, #926-32211) at a final concentration of 0.1 μg/mL for detection of phospho-EB2. Mouse monoclonal anti-total EB2 (Covalab, #mab71717) at 0.81 μg/mL and goat anti-mouse IRDye 680RD (Li-cor, #926-68070) at a final concentration of 0.1 μg/mL were used for detection of total EB2. The nitrocellulose membrane was then scanned on an Odyssey Imager, the phospho-EB2 and total EB2 bands were quantified, and the ratio was calculated.

Golgi-Cox staining

The dendritic morphology of pyramidal cells in the CA1 hippocampal subfield of mice was analyzed following Golgi-Cox staining. Both types of dendrites that are found on pyramidal cells (basal and apical) were analyzed. The samples were processed and analyzed by Neurodigitech (San Diego, CA). A commercially available neuron-tracing software package was used for the digital dendritic reconstruction, followed by dendrograms. During the analyses, animal identifications were kept blinded to the investigators followed by unblinding for the sorting of data and statistical analyses (one-way and two-way ANOVA).

Only spines orthogonal to the dendritic shaft were readily resolved and sampled in this study, whereas spines protruding above or beneath the dendritic shaft were not sampled. The raw data were extrapolated and quantified using the NeuroExplorer program after tracing and spine counting (Microbrightfield, Williston, VT). Sholl analysis was used to characterize the dendritic properties of sampled neurons using a series of concentric circles at 30-μm intervals around the soma. For basal dendrites, analysis spanned 30-μm through 180-μm distances from the soma; for apical dendrites, analysis spanned 30-μm through 210-μm distances from the soma. Within each sphere, the frequency of intersections (or dendritic ramifications), total dendritic length, spine count, and spine density were measured.

Cdkl5 knockout mouse studies

All animal studies were conducted at an Association for Assessment and Accreditation of Laboratory Animal Care (AAALAC)-approved facility under an institutional animal care and use committee (IACUC)-approved protocol. The *Cdkl5* KO mouse line was obtained

Please cite this article in press as: Voronin et al., Preclinical studies of gene replacement therapy for CDKL5 deficiency disorder, Molecular Therapy (2024), https://doi.org/10.1016/j.ymthe.2024.07.012

from The Jackson Laboratory (Bar Harbor, ME), bred in-house, and maintained on the C57BL/6J background (B6.129(FVB)-Cdkl5tm1.1Joez/J, stock #021967).[8] All behavior tests utilized male mice and were conducted under blinded conditions. Study designs utilized Animal Research: Reporting of In Vivo Experiments (ARRIVE) guidelines (https://arriveguidelines.org/arrive-guidelines).

The day of birth was considered PND0. For biodistribution study 1, both male and female homozygous KO mice were used. Heterozygous female *Cdkl5*$^{+/-}$ mice were not utilized. Only male mice were used for behavior (studies 2 and 3). At PND0, mice were anesthetized by inducing hypothermia on wet ice for approximately 5 min (additional details are included in supplemental information). The animals then received a single dose of either vehicle (sterile PBS/0.001% Pluronic F-68) or AAV9.Syn.hCDKL5. Doses were administered bilaterally via i.c.v. injection into the lateral ventricles of the cerebral hemisphere at a volume of 2 μL/hemisphere for a total of 4 μL/whole brain. For i.c.m.-injected mice, animals were injected with 3 μL/whole brain. Doses of AAV9.Syn.hCDKL5 were administered as described in Table 1.

Functional tests

Hindlimb clasp

To assess motor function in male mice, HLC was evaluated. Each mouse was held by its tail approximately 20 cm away from any surface for three consecutive 10-second trials, which were video recorded. Three observers, blinded to treatment, scored the video according to the following scheme: a score of 0 if both limbs remained splayed outward, a score of 1 if a single limb was retracted toward the abdomen, a score of 2 if both limbs were partially retracted toward the abdomen, or a score of 3 if both limbs were entirely retracted or touching the abdomen. Observers documented either the overall score for the three trials or one score per 10-second hold, then averaged.

Open-field test

Mice were subjected to the OFT to examine motor function and anxiety-like behaviors. Mice were brought in their home cages from the vivarium to the testing room and acclimated at least 1 h prior to the test. During the test, mice were placed in the brightly lit open arena (40 cm × 40 cm), one at a time. The locomotive activities of mice were video recorded for 30 min and the data analyzed using the EthoVision system (Noldus Information Technology, Leesburg, VA). The primary parameters included total distance traveled (mobility) and the mobility state. The mobility state was characterized as highly mobile, mobile, and immobile, based upon the number of pixels that changed from one measurement to the next.

Fear conditioning

Fear conditioning was performed to evaluate hippocampal-dependent contextual fear memory. The test included two sessions.

(1) Training. On day 0, animals were trained in a chamber with a wire grid floor that could deliver an electric shock (Noldus/Ugo Basile system). Each mouse was placed in the chamber for 2 min during which mice were actively exploring the new environment and acclimating, after which the first tone (conditioned stimulus [CS]; 30 s, 9 kHz, 80 dB) coincided with a scrambled foot shock 28 s into the tone (unconditioned stimulus [US]; 2 s, 0.5 mA). A total of three CS/US pairings were administered, separated by 1-min intervals. The mouse remained in the chamber for an additional 2 min before being returned to its home cage.
(2) Testing. Fear memory retention was evaluated 24 h after training. Context: the mice were first recorded for 5 min in the same chamber without tone. Freezing behavior was recorded and scored automatically by EthoVision XT15. Freezing was defined as a lack of movement for 2 consecutive seconds or longer.

Nonhuman primate study

Animals, surgeries, necropsy, and tissue processing were conducted on a contractual basis by Labcorp (Madison, WI), as approved by their IACUC. Peripubertal male cynomolgus macaques (*Macaca fascicularis*) were used. At initiation of dosing, animals were 28–37 months old, and body weights ranged from 2.3 to 2.9 kg. Dose formulations were administered with a spinal needle once on day 1 to anesthetized animals by unilateral i.c.v. infusion in the left cerebral ventricle (groups 1 and 2) or bilateral i.c.v. infusion in the left and right cerebral ventricles (group 3). Formulations were delivered via an infusion pump, set to 0.1 mL/min, at a dose volume of 3 mL/dose site (groups 1 and 2) or 1.5 mL/dose site (group 3). Immediately (within 5 min) following the end of the surgical procedure, each animal was placed in a supine position at an approximate 30° incline, with feet elevated above the head while the animal recovered from anesthesia. Each animal was placed in the Trendelenburg position for up to 20 min post completion of dosing.

Assessment of toxicity was based on mortality, clinical observations, body weights, qualitative food consumption, and neurobehavioral observations. Tissues were collected and frozen for analysis of biodistribution using qPCR.

Statistical analysis

Expression and behavioral test data are expressed as mean ± SEM. A one-way ANOVA, with multiple comparisons vs. *Cdkl5* KO vehicle control, was utilized to assess treatment effects. A p value of <0.05 was considered statistically significant. Statistical analysis and graphing were done using GraphPad Prism 10.0.0 (GraphPad Software, San Diego, CA).

To calculate the percent improvement.

(1) For the fear-conditioning tests (where pathology is associated with a decreased value), the following equation was used:

$$\frac{[(\text{Treated} - \text{KO}) \times 100]}{(\text{WT} - \text{KO})},$$

where WT is the value in the wild-type mice and KO is the value in the vehicle-dosed *Cdkl5* KO mice.

(2) For the HLC (where pathology is associated with an increased value), the following equation was used:

$$\frac{[(\text{Treated} - \text{WT}) \times 100]}{(\text{KO} - \text{WT})},$$

where WT is the value in the wild-type mice and KO is the value in the vehicle-dosed *Cdkl5* KO mice.

DATA AND CODE AVAILABILITY

Data are available from the authors upon request.

SUPPLEMENTAL INFORMATION

Supplemental information can be found online at https://doi.org/10.1016/j.ymthe.2024.07.012.

ACKNOWLEDGMENTS

The work reported here was funded by PTC Therapeutics. The authors thank Mary LaRoe, Joseph Colacino, and John Babiak for reviewing the manuscript, and Mark Hemmings for the graphical abstract.

AUTHOR CONTRIBUTIONS

L.C., M.J.K., E.M.W., C.S., and Z.W. designed the gene therapy vector. L.P., E.F., S.S., and Y.V. prepared and quality-controlled the vector. G.V., J.N., M.P., J.P., and M.W. designed the studies and analyzed the data. J.S., J.G., A.M., S.J., P.L., K.S., and J.L. performed the experiments. M.C.W. performed and analyzed the Golgi-Cox staining. P.Y., M.P., and S.D. were responsible for the NHP study and assisted with this research. M.W. wrote the manuscript. B.R., M.P., J.P., Y.V., and J.N. revised and reviewed the final version of the manuscript.

DECLARATION OF INTERESTS

G.V., J.N., J.G., J.S., P.L., M.P., S.D., L.C., Y.V., M.J.K., L.P., E.F., S.S., B.R., P.Y., C.S., J.P., K.S., S.J., J.L., A.M., E.M.W., Z.W., and M.W. are or were at the time the work employees of PTC Therapeutics. M.C.W. is the President and CEO of NeuroDigiTech and was paid by PTC Therapeutics for this work.

REFERENCES

1. Fehr, S., Wilson, M., Downs, J., Williams, S., Murgia, A., Sartori, S., Vecchi, M., Ho, G., Polli, R., Psoni, S., et al. (2013). The CDKL5 disorder is an independent clinical entity associated with early-onset encephalopathy. Eur. J. Hum. Genet. *21*, 266–273.

2. Fehr, S., Wong, K., Chin, R., Williams, S., de Klerk, N., Forbes, D., Krishnaraj, R., Christodoulou, J., Downs, J., and Leonard, H. (2016). Seizure variables and their relationship to genotype and functional abilities in the CDKL5 disorder. Neurology *87*, 2206–2213.

3. Olson, H.E., Demarest, S.T., Pestana-Knight, E.M., Swanson, L.C., Iqbal, S., Lal, D., Leonard, H., Cross, J.H., Devinsky, O., and Benke, T.A. (2019). Cyclin-Dependent Kinase-Like 5 Deficiency Disorder: Clinical Review. Pediatr. Neurol. *97*, 18–25.

4. Rodak, M., Jonderko, M., Rozwadowska, P., Machnikowska-Sokołowska, M., and Paprocka, J. (2022). CDKL5 Deficiency Disorder (CDD)-Rare Presentation in Male. Children (Basel, Switzerland) *9*, 1806.

5. Rusconi, L., Salvatoni, L., Giudici, L., Bertani, I., Kilstrup-Nielsen, C., Broccoli, V., and Landsberger, N. (2008). CDKL5 expression is modulated during neuronal development and its subcellular distribution is tightly regulated by the C-terminal tail. J. Biol. Chem. *283*, 30101–30111.

6. Barbiero, I., De Rosa, R., and Kilstrup-Nielsen, C. (2019). Microtubules: A Key to Understand and Correct Neuronal Defects in CDKL5 Deficiency Disorder? Int. J. Mol. Sci. *20*, 4075.

7. Van Bergen, N.J., Massey, S., Quigley, A., Rollo, B., Harris, A.R., Kapsa, R.M.I., and Christodoulou, J. (2022). CDKL5 deficiency disorder: molecular insights and mechanisms of pathogenicity to fast-track therapeutic development. Biochem. Soc. Trans. *50*, 1207–1224.

8. Wang, I.T.J., Allen, M., Goffin, D., Zhu, X., Fairless, A.H., Brodkin, E.S., Siegel, S.J., Marsh, E.D., Blendy, J.A., and Zhou, Z. (2012). Loss of CDKL5 disrupts kinome profile and event-related potentials leading to autistic-like phenotypes in mice. Proc. Natl. Acad. Sci. USA *109*, 21516–21521.

9. Amendola, E., Zhan, Y., Mattucci, C., Castroflorio, E., Calcagno, E., Fuchs, C., Lonetti, G., Silingardi, D., Vyssotski, A.L., Farley, D., et al. (2014). Mapping pathological phenotypes in a mouse model of CDKL5 disorder. PLoS one *9*, e91613.

10. Okuda, K., Kobayashi, S., Fukaya, M., Watanabe, A., Murakami, T., Hagiwara, M., Sato, T., Ueno, H., Ogonuki, N., Komano-Inoue, S., et al. (2017). CDKL5 controls postsynaptic localization of GluN2B-containing NMDA receptors in the hippocampus and regulates seizure susceptibility. Neurobiol. Dis. *106*, 158–170.

11. Tang, S., Terzic, B., Wang, I.T.J., Sarmiento, N., Sizov, K., Cui, Y., Takano, H., Marsh, E.D., Zhou, Z., and Coulter, D.A. (2019). Altered NMDAR signaling underlies autistic-like features in mouse models of CDKL5 deficiency disorder. Nat. Commun. *10*, 2655.

12. Tang, S., Wang, I.T.J., Yue, C., Takano, H., Terzic, B., Pance, K., Lee, J.Y., Cui, Y., Coulter, D.A., and Zhou, Z. (2017). Loss of CDKL5 in Glutamatergic Neurons Disrupts Hippocampal Microcircuitry and Leads to Memory Impairment in Mice. J. Neurosci. *37*, 7420–7437.

13. Gao, Y., Irvine, E.E., Eleftheriadou, I., Naranjo, C.J., Hearn-Yeates, F., Bosch, L., Glegola, J.A., Murdoch, L., Czerniak, A., Meloni, I., et al. (2020). Gene replacement ameliorates deficits in mouse and human models of cyclin-dependent kinase-like 5 disorder. Brain *143*, 811–832.

14. Liguore, W.A., Domire, J.S., Button, D., Wang, Y., Dufour, B.D., Srinivasan, S., and McBride, J.L. (2019). AAV-PHP.B Administration Results in a Differential Pattern of CNS Biodistribution in Non-human Primates Compared with Mice. Mol. Ther. *27*, 2018–2037.

15. Medici, G., Tassinari, M., Galvani, G., Bastianini, S., Gennaccaro, L., Loi, M., Mottolese, N., Alvente, S., Berteotti, C., Sagona, G., et al. (2022). Expression of a Secretable, Cell-Penetrating CDKL5 Protein Enhances the Efficacy of Gene Therapy for CDKL5 Deficiency Disorder. Neurotherapeutics *19*, 1886–1904.

16. Jakimiec, M., Paprocka, J., and Śmigiel, R. (2020). CDKL5 Deficiency Disorder-A Complex Epileptic Encephalopathy. Brain Sci. *10*, 107.

17. Baltussen, L.L., Negraes, P.D., Silvestre, M., Claxton, S., Moeskops, M., Christodoulou, E., Flynn, H.R., Snijders, A.P., Muotri, A.R., and Ultanir, S.K. (2018). Chemical genetic identification of CDKL5 substrates reveals its role in neuronal microtubule dynamics. EMBO J. *37*, e99763.

18. DeGennaro, L.J., Kanazir, S.D., Wallace, W.C., Lewis, R.M., and Greengard, P. (1983). Neuron-specific phosphoproteins as models for neuronal gene expression. Cold Spring Harb. Symp. Quant. Biol. *48*, 337–345.

19. Okuda, K., Takao, K., Watanabe, A., Miyakawa, T., Mizuguchi, M., and Tanaka, T. (2018). Comprehensive behavioral analysis of the Cdkl5 knockout mice revealed significant enhancement in anxiety- and fear-related behaviors and impairment in both acquisition and long-term retention of spatial reference memory. PLoS One *13*, e0196587.

20. Ayers, J.I., Fromholt, S., Sinyavskaya, O., Siemienski, Z., Rosario, A.M., Li, A., Crosby, K.W., Cruz, P.E., DiNunno, N.M., Janus, C., et al. (2015). Widespread and efficient transduction of spinal cord and brain following neonatal AAV injection and potential disease modifying effect in ALS mice. Mol. Ther. *23*, 53–62.

21. Lukashchuk, V., Lewis, K.E., Coldicott, I., Grierson, A.J., and Azzouz, M. (2016). AAV9-mediated central nervous system-targeted gene delivery via cisterna magna route in mice. Mol. Ther. Methods Clin. Dev. *3*, 15055.

22. Kügler, S., Kilic, E., and Bähr, M. (2003). Human synapsin 1 gene promoter confers highly neuron-specific long-term transgene expression from an adenoviral vector in the adult rat brain depending on the transduced area. Gene Ther. *10*, 337–347.

23. Terzic, B., Davatolhagh, M.F., Ho, Y., Tang, S., Liu, Y.T., Xia, Z., Cui, Y., Fuccillo, M.V., and Zhou, Z. (2021). Temporal manipulation of Cdkl5 reveals essential post-developmental functions and reversible CDKL5 deficiency disorder-related deficits. J. Clin. Invest. *131*, e143655.

24. Kind, P.C., and Bird, A. (2021). CDKL5 deficiency disorder: a pathophysiology of neural maintenance. J. Clin. Invest. *131*, e153606.

25. Ge, W.P., Miyawaki, A., Gage, F.H., Jan, Y.N., and Jan, L.Y. (2012). Local generation of glia is a major astrocyte source in postnatal cortex. Nature *484*, 376–380.

26. Lalonde, R., and Strazielle, C. (2011). Brain regions and genes affecting limb-clasping responses. Brain Res. Rev. *67*, 252–259.

27. Ta, D., Downs, J., Baynam, G., Wilson, A., Richmond, P., and Leonard, H. (2022). A brief history of MECP2 duplication syndrome: 20-years of clinical understanding. Orphanet J. Rare Dis. *17*, 131.

28. Bolton, P.F., Dennis, N.R., Browne, C.E., Thomas, N.S., Veltman, M.W., Thompson, R.J., and Jacobs, P. (2001). The phenotypic manifestations of interstitial duplications of proximal 15q with special reference to the autistic spectrum disorders. Am. J. Med. Genet. *105*, 675–685.

29. Szafranski, P., Golla, S., Jin, W., Fang, P., Hixson, P., Matalon, R., Kinney, D., Bock, H.G., Craigen, W., Smith, J.L., et al. (2015). Neurodevelopmental and neurobehavioral characteristics in males and females with CDKL5 duplications. Eur. J. Hum. Genet. *23*, 915–921.

30. Frasca, A., Pavlidou, E., Bizzotto, M., Gao, Y., Balestra, D., Pinotti, M., Dahl, H.A., Mazarakis, N.D., Landsberger, N., and Kinali, M. (2022). Not Just Loss-of-Function Variations: Identification of a Hypermorphic Variant in a Patient With a CDKL5 Missense Substitution. Neurol. Genet. *8*, e666.

31. Hector, R.D., Dando, O., Ritakari, T.E., Kind, P.C., Bailey, M.E.S., and Cobb, S.R. (2017). Characterisation of Cdkl5 transcript isoforms in rat. Gene *603*, 21–26.